Modular patterning of structure and function of the striatum by retinoid receptor signaling

Wen-Lin Liao*, Hsiu-Chao Tsai*, Hsiao-Fang Wang*, Josephine Chang*, Kuan-Ming Lu*, Hsiao-Lin Wu*, Yi-Chao Lee[†], Ting-Fen Tsai[‡], Hiroshi Takahashi[§], Michael Wagner[¶], Norbert B. Ghyselinck[‖], Pierre Chambon[‖]**, and Fu-Chin Liu*,**[††]

*Institute of Neuroscience, [††]Center of Neuroscience, [‡]Department of Life Sciences, National Yang-Ming University, Taipei, Taiwan 112, Republic of China; [†]Center for Gene Regulation and Signal Transduction Research, National Cheng Kung University, Tainan, Taiwan 701, Republic of China; [§]Developmental Neurobiology Group, Mitsubishi Kagaku Institute of Life Sciences, Tokyo, 194-8511, Japan; [¶]Department of Anatomy and Cell Biology, College of Medicine, State University of New York Health Science Center, Brooklyn, NY 11203; and [‖]Institut de Génétique et de Biologie Moléculaire et Cellulaire (IGBMC), Centre National de la Recherche Scientifique/Institut National de la Santé et de la Recherche Médicale/University Louis Pasteur, Collège de France, 67404 Illkirch Cedex, CU de Strasbourg, France

Contributed by Pierre Chambon, March 2, 2008 (sent for review December 21, 2007)

Retinoid signaling plays a crucial role in patterning rhombomeres in the hindbrain and motor neurons in the spinal cord during development. A fundamentally interesting question is whether retinoids can pattern functional organization in the forebrain that generates a high order of cognitive behavior. The striatum contains a compartmental structure of striosome (or ''patch'') and intervening matrix. How this highly complex mosaic design is patterned by the genetic programs during development remains elusive. We report a developmental mechanism by which retinoid receptor signaling controls compartmental formation in the striatum. We analyzed RAR$\beta^{-/-}$ mutant mice and found a selective loss of striosomal compartmentalization in the rostral mutant striatum. The loss of RARβ signaling in the mutant mice resulted in reduction of cyclin E2, a cell cycle protein regulating transition from G_1 to S phase, and also reduction of the proneural gene *Mash1*, which led to defective neurogenesis of late-born striosomal cells. Importantly, during striatal neurogenesis, endogenous levels of retinoic acid were spatiotemporally regulated such that transduction of high levels of retinoic acid through RARβ selectively expanded the population of late-born striosomal progenitors, which evolved into a highly elaborate compartment in the rostral striatum. RAR$\beta^{-/-}$ mutant mice, which lacked such enlarged compartment, displayed complex alternations of dopamine agonist-induced stereotypic motor behavior, including exaggeration of head bobbing movement and reduction of rearing activity. RARβ signaling thus plays a crucial role in setting up striatal compartments that may engage in neural circuits of psychomotor control.

basal ganglia | cell proliferation | retinoic acid | stereotypic behavior

A general principle of functional organization in the central nervous system is the compartmental arrangement of neuronal populations. The columnar organization of the cerebral cortex represents the most elaborate compartmental organization in the telencephalon, but compartmental organization also is present in the striatum. The striatum comprises two neurochemically distinct compartments, striosome (or patch) and the matrix (1–3). Unlike the columnar organization of the cerebral cortex, striosomes, which comprise ≈15–20% of the striatum, are embedded in the surrounding matrix to form a labyrinthine structure. Neurons in striosomes and in the matrix are generated during different time windows, differentiate at different rates into different neurochemical phenotypes, establish different connectivity with other brain regions, and degenerate at different rates in neurodegenerative diseases (2, 3).

Retinoid signaling, by virtue of its powerful patterning ability in developmental control, is involved in specification of body axis and building structural organs (4). Retinoid signaling plays a crucial role in patterning rhombomeres in the hindbrain and motor neurons in the spinal cord during development (5). A fundamentally interesting question is whether retinoids can pattern functional organization in the forebrain that generates cognitive behavior. Previous studies have shown that development of the intermediate part of telencephalon, which gives rise to the striatum in the mammalian telencephalon, is regulated by retinoid signaling (6–10). It is, however, unknown whether retinoid signaling is involved in control of compartmental formation during striatal development.

Retinoid signaling is transduced by binding to retinoic acid (RA) receptors (RARα, RARβ, RARγ) and retinoid X receptors (RXRα, RXRβ, RXRγ) that belong to the steroid/thyroid receptor superfamily (4). RARs and RXRs are ligand-activated transcription factors that can transactivate downstream target genes. Of the different subtypes of RARs, RARβ is preferentially expressed in the developing striatum (11–13). We report in the present study that RARβ signaling plays a critical role in setting up striatal compartmentation by differential regulation of the population sizes of striosomal cells along the rostrocaudal axis during development, and the enlarged striosomal compartment in the rostral striatum may modulate the neural circuits of psychomotor function.

Results

Aberrant Compartmentation in the Striatum of RAR$\beta^{-/-}$ Mutant Mice. Striosomes express high levels of μ-opioid receptor (MOR1) and dynorphin but low levels of calbindin-D_{28K} and met-enkephalin [Fig. 1 *A* and *C*; supporting information (SI) Fig. S1 *A* and *C*] (2, 3). MOR1 immunostaining showed that the areas of MOR1-positive striosomes were drastically reduced by 71.1% in RAR$\beta^{-/-}$ mutant striatum (Fig. 1 *A*, *A′*, and *F*). MOR1-positive striosomes disappeared mainly in the rostral striatum (Fig. 1 *A*, *A′*, and *F*) but were largely spared in the ventromedial striatum at middle and caudal levels (Fig. 1 *B*, *B′*, and *F*). Dynorphin was also reduced in the rostral mutant striatum (Fig. S1 *A*, *A′*, and *F*). Moreover, calbindin-poor zones (striosomes) were drastically diminished in the rostral striatum such that calbindin expression became largely homogeneous (Fig. 1 *C′* and *E′*). The number of calbindin-positive neurons was, however, not significantly altered in mutant striatum (wild type, 1,315.5 ± 372.2/mm^2; mutant, 1,297.0 ± 315.6/mm^2, $P = 0.887$, $n = 3$). Immunostaining of met-enkephalin showed similar results to that of calbindin (Fig. S1 *C*, *C′*, *E*, and *E′*). Notably, in addition to the changes of striosomal markers, the striatal area was decreased in the rostral but not the caudal mutant striatum (Fig. 1*G*), suggesting a cytoarchitectural change. The perinatal strio-

Author contributions: W.-L.L. and F.-C.L. designed research; W.-L.L., H.-C.T., H.-F.W., J.C., K.-M.L., H.-L.W., and Y.-C.L. performed research; T.-F.T., H.T., M.W., N.B.G., and P.C. contributed new reagents/analytic tools; W.-L.L., H.-F.W., and F.-C.L. analyzed data; and W.-L.L. and F.-C.L. wrote the paper.

The authors declare no conflict of interest.

**To whom correspondence may be addressed. E-mail: chambon@titus.u-strasbg.fr or fuchin@ym.edu.tw.

This article contains supporting information online at www.pnas.org/cgi/content/full/0802109105/DCSupplemental.

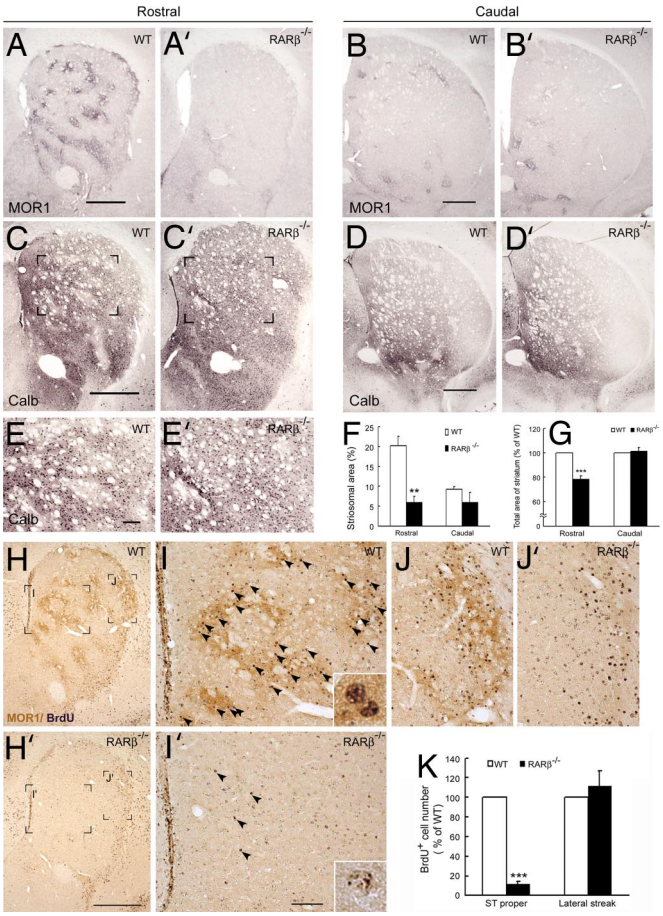

Fig. 1. Aberrant compartments of striosomes and matrix in the adult striatum of RAR$\beta^{-/-}$ mutant mice. Immunostains of MOR1 (*A*, *A′*, *B*, *B′*) and calbindin (*C*, *C′*, *D*, *D′*) show that striosomes, as marked by MOR1-positive neuropil patches (*A*) and calbindin-poor zones (*C*), are reduced in the mutant striatum at rostral levels (*A′*, *C′*). The bracketed regions in *C*, *C′* are shown at high magnification in *E*, *E′*. The areas of MOR1-positive patches are decreased in RAR$\beta^{-/-}$ mutant mice at the rostral level (*F*). The striosomal reduction of MOR1 and loss of calbindin-poor zones are less prominent in the mutant striatum at caudal levels (*B*, *B′*, *D*, *D′*, *F*). (*G*) The striatal area was reduced at the rostral but not the caudal level. (*H–K*) Loss of late-born S cells in RAR$\beta^{-/-}$ mutant striatum. The bracketed regions in *H*, *H′* are shown at high magnification in *I*, *I′*, *J*, *J′*. Double immunostaining of MOR1 and BrdU (*H–J′*) shows that S cells pulse-labeled with BrdU at E12.75 and E13 (darkly stained black nuclei, arrowheads) are typically concentrated in MOR1-positive striosomes (brown neuropil patches, *H*, *I*) and the subcallosal lateral streak (*H* and *J*) in wild-type striatum. In contrast, only a few darkly stained BrdU-positive S cells (arrowheads) are present in the mutant striatum (*H′*, *I′*). BrdU-labeled cells are illustrated at high magnification in *Insets* (*I*, *I′*). Note that BrdU-positive S cells remain in the subcallosal lateral streak of mutant striatum (*J′*). (*K*) The number of BrdU-positive S cells is decreased in the striatal proper of mutant striatum but not in the lateral streak. **, $P < 0.01$, ***, $P < 0.001$, Student's *t* test, $n = 3$. (Scale bars in *A* for *A*, *A′*, 500 μm; in *B* for *B*, *B′*, 500 μm; in *C* for *C*, *C′*, 500 μm; in *D* for *D*, *D′*, 500 μm; in *E* for *E*, *E′*, 200 μm; In *H′* for *H*, *H′* 500 μm; in *I′* for *I–J′*, 100 μm.)

somes express high levels of MOR1, dopamine- and cyclic adenosine 3′:5′-monophosphate-regulated phosphoprotein (DARPP-32), and tyrosine hydroxylase (TH). These three markers were also reduced primarily in the rostral part of newborn mutant striatum (Fig. S2 *A–J′*). *Ebf-1*, a marker for developing matrix (14), was increased in the rostral but not in the caudal part of newborn mutant striatum (Fig. S2 *K–M*). Defective striosomes also occurred prenatally at E16.5. At E16.5, DARPP-32-positive neurons were not yet organized into striosomal pattern in the wild-type striatum, but DARPP-32 neurons were significantly reduced in the mutant striatum (Fig. S3 *B* and *B′*), which indicated that the reduction of striosomes occurred before compartmental formation.

Loss of Late-Born Striosomal Neurons in RAR$\beta^{-/-}$ Mutant Mice. The concurrent decreases of several striosomal markers suggested that RARβ-null mutation might affect neurogenesis and/or survival of striosomal neurons. Striosomal cells (S cells) and matrix cells (M cells) finish their last mitosis at different time windows (15, 16). The majority of S and M cells can be pulse-labeled with BrdU at E11.5–E13.5 and after E16.5, respectively, in the mouse. Within the S cell population, most S cells in the caudal striatum and the subcallosal lateral streak are born at E11–E12.5, whereas most S cells in the rostral striatum are born later at E12.5–E13.5 in the mouse (17) (W.-L.L. and F.-C.L., unpublished observations).

Because RARβ mutation-induced decreases of S markers primarily occurred in the rostral striatum, we pulse-labeled rostral S cells with two injections of BrdU at E12.75 and E13. Clusters of BrdU-labeled S cells were drastically reduced by 88.2% in the rostral RAR$\beta^{-/-}$ mutant striatum (Fig. 1 *H*, *H′*, *I*, *I′*, and *K*). Similar findings were observed in the newborn mutant striatum (Fig. S3 *A*, *A′*, *C*, and *C′*). The subcallosal lateral streak, which comprised early-born S cells, remained largely unaffected in the rostral mutant striatum (Fig. 1 *J*, *J′*, and *K*). Importantly, the loss of late-born S cells occurred at E12.75 before the segregation of S and M cells into compartments, because the reduction of BrdU-labeled cells was detected in the mutant lateral ganglionic eminence (LGE, striatal anlage) at 28 h postinjection of BrdU when the BrdU-labeled postmitotic cells had migrated into the differentiated mantle zone but were not yet organized into compartments (Fig. 2 *A*, *A′*, and *C*).

Defective Neurogenesis of Late-Born Striosomal Cells in Striatal Anlage of RAR$\beta^{-/-}$ Mutant Embryos. The loss of late-born S cells in the mutant striatum might be due to aberrant cell death and/or defective neurogenesis induced by RARβ-null mutation. We assayed cell death by TUNEL staining. The number of apoptotic cells in the wild-type LGE did not significantly differ from that in the mutant LGE at E12.75, E13.5, E14.5, and E15.5 (Fig. S4), which ruled out cell death as the primary cause of cell loss.

In addition to the mantle zone, low levels of RARβ were expressed in the ventricular zone (VZ) of LGE as detected by RT-PCR and *in situ* hybridization (Fig. S5), which is consistent with the report that RARβ is expressed by proliferating progenitors in neurospheres derived from striatal anlage (18). To determine whether the reduction of S cells was due to defective proliferation of S progenitors in the germinal zones, we pulse-labeled late-born S progenitors with BrdU at E12.75 and examined the BrdU incorporation rate at 1 h after BrdU injection. BrdU-positive cells were reduced by 16.7% in the VZ of RAR$\beta^{-/-}$ mutant LGE (Fig. 2 *B* and *B′*, *D*, and *E*). The reduction was specific to the LGE, because it did not occur in the ventral pallium of cortical anlage (Fig. 2*E*). In parallel to the defective proliferation, cyclin E2 (Ccne2), a cell cycle protein regulating transition from G_1 to S phase (19), was decreased by 16.1% in the mutant LGE (Fig. 2 *F*, *F′*, and *H*). Moreover, the proneural gene *Mash1* was also reduced by 19.3% in the mutant LGE (Fig. 2 *G*, *G′*, and *I*). BrdU-positive cells tended to decrease in the mutant subventricular zone (SVZ), a secondary proliferative population in the germinal zones (86.2 ± 7.5% of wild type, $P = 0.0718$, $n = 6$).

The deficit in cell proliferation was specific to late-born S cells, because pulse labeling of early-born S cells at E11.5 or M cells at E16.5 with BrdU did not show significant differences of BrdU-positive cells in the LGE/developing striatum between the wild-type and RAR$\beta^{-/-}$ mutant embryos (Fig. 2*D*). These results are in good accordance with the aforementioned findings that early-born S cells and M cells were spared in the adult mutant striatum (Fig. 1 *F* and *K*). Note that the loss of late-born S progenitors was not due to depletion of precursor pools by precocious differentiation, because no apparent increase of TuJ1-positive neurons was observed in E12.75 and E13.5 mutant LGE (data not shown).

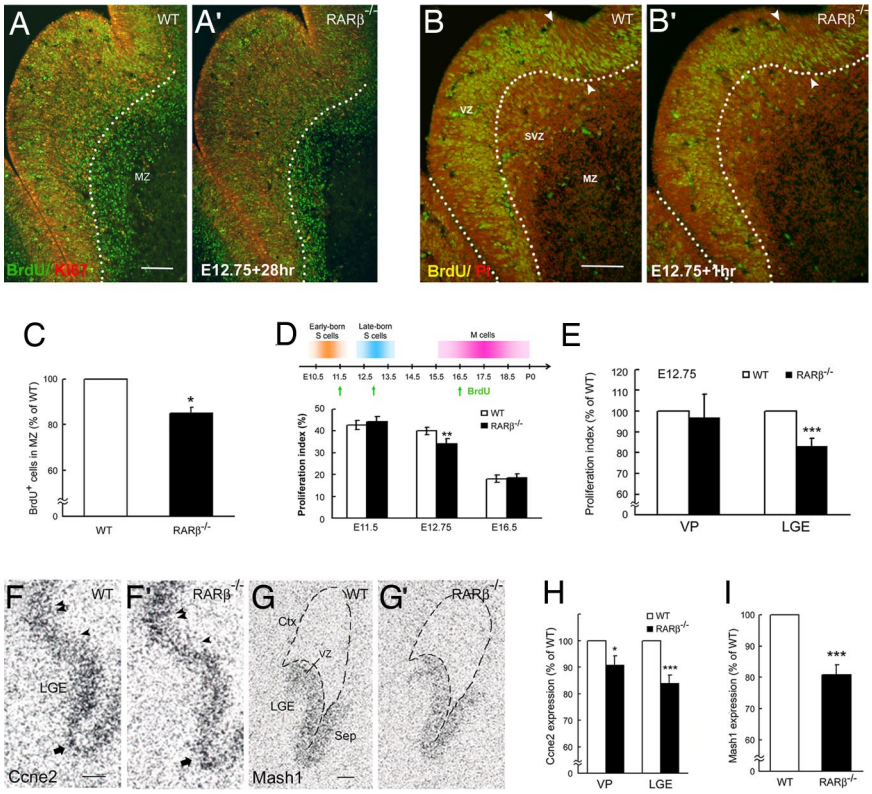

Fig. 2. Defective neurogenesis of late-born S cells in striatal anlage of RARβ$^{-/-}$ mutant embryos. (*A*, *A′*, *C*) Twenty-eight hours after a single pulse labeling of BrdU at E12.75, more BrdU-positive S cells (green) migrate into the Ki67-negative differentiated mantle zone (MZ) of wild-type LGE (*A*) than that in the mutant LGE (*A′*, *C*). (*B*, *B′*, *D*, *E*) The number of S cells pulse-labeled with BrdU for 1 h at E12.75 is reduced in the VZ of LGE but not in the VP (*E*). The arrowheads in *B*, *B′* indicate the boundary between the LGE and the VP. The reduction of cell proliferation also is temporally specific, because it occurs only in the S progenitor pulse-labeled with BrdU at E12.75 (late-born S cells) but not at E11.5 (early-born S cells; *D*), nor does it occur in the progenitors of matrix (M) cells pulse-labeled with BrdU at E16.5 (*D*). (*F–I*) Reduction of neurogenesis markers in RARβ$^{-/-}$ mutant LGE. *Ccne2* mRNA is decreased in the mutant E12.75 LGE and VP (*F*, *F′*, *H*). The VP and the LGE are indicated by the regions between the double and single arrowheads and between the single arrowhead and arrow, respectively, in *F*, *F′*. *Mash1* mRNA is reduced in E13.5 RARβ$^{-/-}$ mutant LGE (*G*, *G′*, *I*). *, $P < 0.05$; ***, $P < 0.001$, Student's *t* test. All experiments were repeated at least three times. CTX, cortex; Sep, septum; SVZ, subventricular zone; VP, ventral pallium. (Scale bars in *A* for *A*, *A′*; in *B* for *B*, *B′*; in *F* for *F*, *F′*; and in *G* for *G*, *G′*, 100 μm.)

RA Increased Cell Proliferation of Striatal Progenitors. It remained a puzzle within the S cell population why RARβ mutation primarily targeted the late-born S cells, whereas it relatively spared the early-born S cells. A possible account for this differential effect is that the early-born S cells might be incompetent to transduce RA signals. To test this hypothesis, wild-type mouse embryos were maternally treated with all-trans RA (5 mg/kg) every 12 h from E10.5 to E11.5 and then pulse-labeled with BrdU for 1 h before embryo culling. The RA treatments resulted in increases of BrdU-positive cells in the VZ of LGE at rostral, middle, and caudal levels (Fig. 3 *B*, *B′*, and *E*) and decreases of TuJ1-positive areas in the mantle zone (Fig. 3 *B* and *B′*). These results indicated that early-born S progenitors were in fact competent to transduce RA signals by expanding its population.

To further test whether the RA-enhanced cell proliferation was mediated through RARβ signaling, the same set of experiments were performed in RARβ$^{-/-}$ mutant embryos and their wild-type littermates. RA treatments did not effectively increase proliferation of early-born S cells in RARβ$^{-/-}$ mutant LGE at rostral and middle levels (Fig. 3*F*), which indicated that the lack of RARβ largely prevented RA from increasing proliferation of early-born S cells.

We also tested whether exogenous RA could alter proliferation of late-born S cells by maternally treating wild-type mouse embryos with RA every 12 h from E12.5 to E13.5 and then pulse-labeling with BrdU for 1 h before culling. The RA treatments did not alter cell proliferation in the rostral and middle parts of E13.5 LGE (Fig. 3*G*). We surmised that this might be due to high levels of endogenous RA present in the rostral/middle LGE at E12.5–E13.5, which could limit the effect of exogenous RA (see below, Fig. 4 *B*, *E*, and *H*). Accordingly, RA induced-cell proliferation should occur in the region where endogenous RA was low. Indeed, exogenous RA increased BrdU-positive cells in the VZ of caudal part of E13.5 LGE (Fig. 3 *D*, *D′*, and *G*), where a low level of endogenous RA was present (see below, Fig. 4 *C*, *F*, and *I*).

Chronic RA Treatments Resulted in Enlarged Caudal Striosomes. We further assayed the effects of chronic RA treatments during the entire neurogenesis of S and M cells. The embryos treated with RA every 12 h from E11.5 to E17.5 had enlarged DARPP-32- and GluR1-positive striosomes in the caudal striatum (Fig. S6). No significant effect was observed in rostral striosomes, which contained late-born S cells, nor did the population of M cells appear to be affected by the RA treatments (data not shown). Because striosomes in the caudal striatum were made up of early-born S cells, these results were consistent with the findings that exogenous RA mainly increased proliferation of early-born S cells (Fig. 3 *B*, *B′*, and *E*) and further suggest that as a consequence, more early-born S cells are recruited to caudal striosomes.

RA Directly Regulated Proliferation of Striatal Progenitor-Derived Cells *in Vitro*. To further determine whether RA could directly regulate proliferation of striatal progenitors, we used the ST14A cell line, which was immortalized from rat striatal progenitors during the neurogenesis time window of S cells at E14 (20). The proliferating ST14A cells expressed RARβ and RXRβ transcripts (Fig. S7*D*). All-trans RA (1 μM) increased proliferation of ST14A cells, because BrdU-labeled cells were significantly increased by 142.3% with RA treatment (Fig. S7 *B* and *C*). RA also increased *Ccne2* and decreased the differentiation marker of microtubule-associated protein 2 (Fig. S7*D*).

Spatiotemporal Regulation of Endogenous Levels of RA in Striatal Anlage. Given that early-born S cells are capable of responding to RA signals, why is this cell population less affected by RARβ mutation? We postulated that the concentration of RA might be very low in E10.5–E11.5 LGE when the early-born S cells undergo neurogenesis. During early telencephalic development, a major RA source for the LGE is synthesized by retinaldehyde dehydrogenase 3 (Raldh3) (10, 21), although Raldh1 is present in the mesostriatal afferents (22). We found that few cells expressing *Raldh3* mRNA were present in E11.5 LGE (Fig. 4*A*). In contrast, when the late-born S cells undergo neurogenesis at E12.5–E13.5, many *Raldh3*-positive cells were present in the rostral/middle LGE but

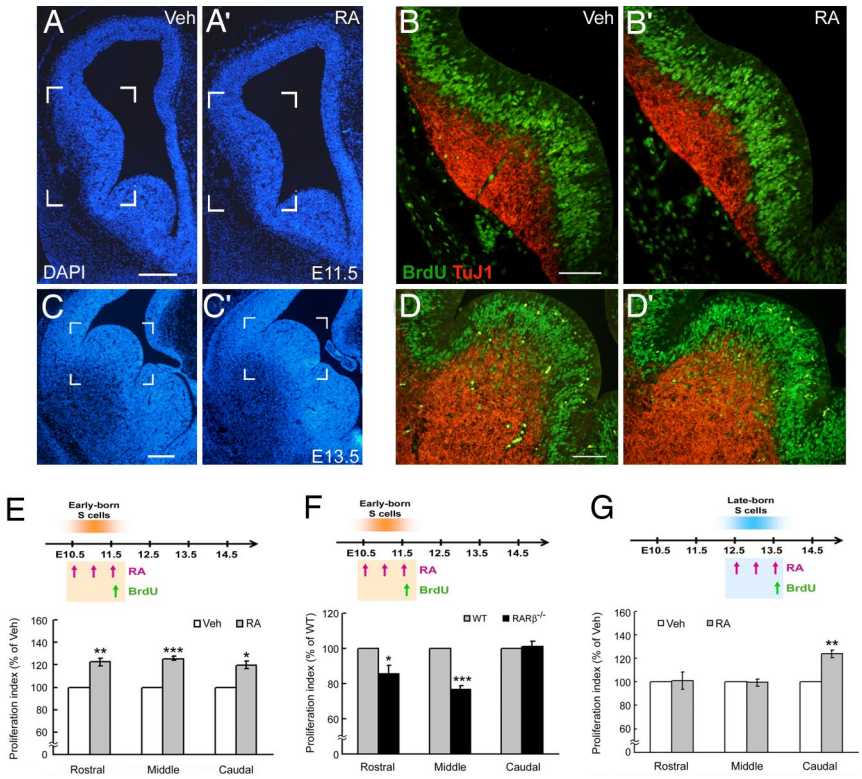

Fig. 3. RA-induced increases of cell proliferation in striatal anlage. Embryos were maternally treated with all-trans RA (5 mg/kg) every 12 h from E10.5 to E11.5 (*A*, *A*′, *B*, *B*′, *E*, *F*) or E12.5 to E13.5 (*C*, *C*′, *D*, *D*′, *G*) and were then pulse-labeled with BrdU for 1 h before culling. RA treatments during E10.5–E11.5 result in increases of BrdU-positive cells (green nuclei) in the rostral, middle, and caudal levels of E11.5 wild-type LGE (*B*, *B*′, *E*), but not in RAR$\beta^{-/-}$ mutant LGE at the rostral and middle levels (*F*). The RA treatments during E12.5–E13.5 resulted in increases of BrdU-positive cells in the caudal (*D*, *D*′, *G*) but not the rostral and middle LGE (*G*). The bracketed regions in *A*, *A*′, *C*, *C*′ are shown at high magnification in *B*, *B*′, *D*, *D*′, respectively. *, $P < 0.05$; **, $P < 0.01$, ***, $P < 0.001$, Student's *t* test. All experiments were repeated at least three times. (Scale bars in *A* for *A*, *A*′, 200 μm; in *B* for *B*, *B*′, 100 μm; in *C* for *C*, *C*′, 200 μm; and in *D* for *D*, *D*′, 100 μm.)

not in the caudal LGE (Fig. 4 *B* and *C*) (21). We further determined the endogenous RA level in the LGE with a coculture assay. Using the Sil-15 RA reporter cells, RA produced by explant tissue could be detected by activation of the β-galactosidase reporter gene (9, 23). Few X-gal-positive cells were found when cocultured with E11.5 LGE (Fig. 4 *D* and *G*). In contrast, many X-gal-positive cells were detected when cocultured with the rostral (Fig. 4 *E* and *H*) but not the caudal part of E13.5 LGE (Fig. 4 *F* and *I*). These results confirmed that endogenous RA in the LGE was very low during the neurogenesis time window of early-born S cells, whereas a substantial level of RA was present during the neurogenesis time window of late-born S cells in the rostral LGE.

Alterations of Dopamine Agonist-Induced Stereotypic Motor Behaviors in RAR$\beta^{-/-}$ Mutant Mice. The selective loss of rostral striosomes in RAR$\beta^{-/-}$ mutant mice provided a unique opportunity to look into the functional significance of S compartments at the behavioral level. We treated the mice with apomorphine, a stereotypy-eliciting dopamine agonist, and examined the stereotypic motor behaviors, including head bobbing, rearing, and grooming. With the vehicle treatment, wild-type and mutant mice had similar activities of locomotion, head movement, rearing, and grooming (Fig. 5 *A*–*C*; data not shown). Apomorphine (3 mg/kg) increased the locomotor activity in wild-type and RAR$\beta^{-/-}$ mutant mice to similar degrees (Fig. 5*A*). Apomorphine at the dosage of 3 mg/kg was ineffective in inducing repeated head bobbing in wild-type mice, but it drastically induced stereotypic head-bobbing movement in RAR$\beta^{-/-}$ mutant mice at 20 and 50 min after injection ($P < 0.001$, two-way ANOVA; Fig. 5*B*), which suggested the head-bobbing behavior was exaggerated in RAR$\beta^{-/-}$ mutant mice. Apomorphine at 3 mg/kg was also ineffective in altering the rearing activity in wild-type mice (Fig. 5*C*), but the rearing activity was completely lost in RAR$\beta^{-/-}$ mutant mice at 20 min after apomorphine injection ($P < 0.001$, two-way ANOVA; Fig. 5*C*). The grooming activity tended to decrease in apomorphine-treated RAR$\beta^{-/-}$ mutant mice, but the decrease did not reach statistical significance (data not shown).

Discussion

Our study provides previously undescribed genetic evidence that retinoid receptor signaling plays a crucial role in patterning the functional organization in the striatum that is involved in generation

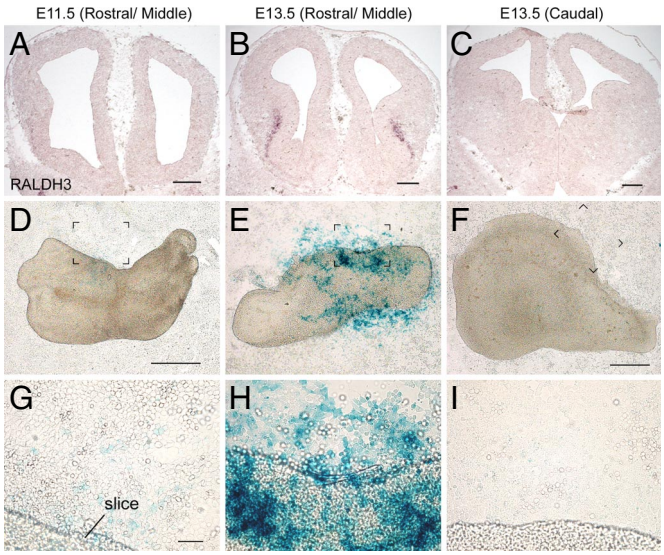

Fig. 4. Spatiotemporal regulation of endogenous RA in the LGE. None or at most few Raldh3-positive cells are present in E11.5 LGE (*A*). By E13.5, many Raldh3-positive cells are present in the rostral/middle part of LGE (*B*), but few Raldh3-positive cells are present in the caudal LGE (*C*). (*D*–*I*) Detection of endogenous RA in the LGE with the RA reporter cells assay. Few X-gal-positive Sil-15 reporter cells are present in the coculture of E11.5 LGE (*D* and *G*) or the caudal part of E13.5 LGE (*F* and *I*), whereas many X-gal-positive reporter cells are present in the coculture of rostral/middle part of E13.5 LGE (*E* and *H*). The bracketed regions in *D*–*F* are shown at high magnification in *G*–*I*, respectively. (Scale bars, in *A*–*C*, 200 μm; in *D* for *D*, *E*, 500 μm; in *F*, 500 μm; and in *G* for *G*–*I*, 50 μm.)

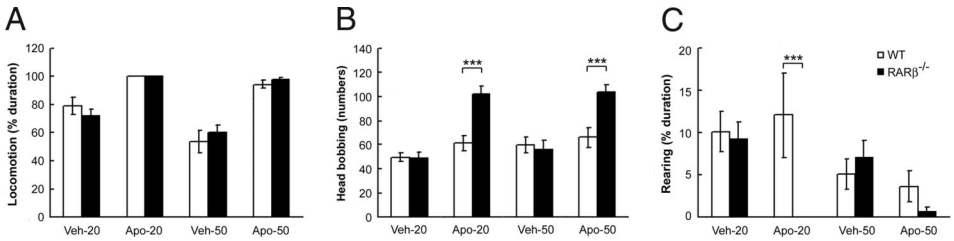

Fig. 5. Behavioral analyses of RAR$\beta^{-/-}$ mutant mice. (*A*) The locomotor activity of RAR$\beta^{-/-}$ mutant mice does not differ from wild-type mice either with the challenges of vehicle or apomorphine (Apo, 3 mg/kg) at 20 and 50 min after drug injections. (*B*) Apomorphine significantly increases the head-bobbing movement in RAR$\beta^{-/-}$ mutant mice at 20 and 50 min after the drug injection compared with wild-type mice. Note that apomorphine at this low dose does not increase head bobbing in wild-type mice. (*C*) Apomorphine (3 mg/kg) completely inhibited the rearing activity of RAR$\beta^{-/-}$ mutant mice at 20 min after injection. ***, $P < 0.001$, two-way ANOVA, Bonferroni's post hoc test. Apo-20, Apo-50, Veh-20, Veh-50: 20 and 50 min after the injections of apomorphine or its vehicle.

of psychomotor behavior. Our experiments demonstrate heterogeneity of S cell populations along the rostrocaudal axis in terms of RARβ signaling. The population of late-born S cells, which is preferentially expanded by high levels of RA through RARβ signaling to form a large S compartment in the rostral striatum, may engage in modulating neural circuits of psychomotor function.

Regulation of Proliferation of S Progenitors by RARβ Signaling. RARβ mutation resulted in defective proliferation of late-born S cells. In addition to the differentiated mantle zone, RARβ is expressed at low levels in the progenitor domains of LGE (Fig. S5) and by progenitor cells in neurospheres derived from striatal anlage (18). The expression of RARβ in striatal progenitors suggests a cell-autonomous effect of RARβ in regulating proliferation of striatal progenitors, which is corroborated by our finding that RA increased proliferation of striatal progenitors-derived ST14A cells. A previous cell lineage study has suggested a heterogeneity of S and M progenitors within the proliferative VZ (24). It is likely that both the late-born S progenitors and the M progenitors were concurrently labeled by the 1-hour pulse of BrdU at E12.75 LGE. Because the population of M cells is the dominant population in the striatum (≈80–85% of total striatal neurons) and the neurogenesis of M cells was not affected by RARβ mutation, the RARβ mutation-induced moderate decreases in cell proliferation and *Ccne2* and *Mash1* mRNA levels are likely to reflect a selectivity of defective neurogenesis of the small population of late-born S progenitors. The presence of low levels of RARβ in the progenitor domains may thus suggest a selective expression of RARβ in a small population of S progenitors.

A Stage-Dependent Dual Mode of RA Signaling for Controlling Striatal Development. It is unclear why the proliferation of M progenitor cells was unaffected in RAR$\beta^{-/-}$ mutant LGE, which may be due to the absence of RARβ or selective expression of RA degrading enzymes in M progenitors. Unlike M progenitor cells, differentiating M cells were competent for transducing RA signals, because *Ebf-1*, a differentiating marker of M cells (14), was increased in RAR$\beta^{-/-}$ striatum, suggesting that differentiation of M cells is regulated by RARβ signaling. RA signaling has been shown to regulate differentiation of striatal molecules, particularly the molecules involved in dopamine signal transduction including D1 and D2 receptors and DARPP-32 (6, 10, 12, 25–28). Given that most RA-regulated dopamine signaling molecules are first expressed by S and also later by M cells during development, we propose a stage-dependent dual mode of RA signaling in which RA first regulates proliferation of late-born S progenitors and later differentiation of postmitotic S and M cells in striatal development.

Patterning the Labyrinthine of Striatal Compartments by RARβ Signaling. The S compartments, as shown by 3D reconstruction study, form a labyrinthine structure in which the S compartment is larger and more elaborate at the rostral than the middle and caudal levels (29). Given the differentially proliferating effects by RA on S cells undergoing neurogenesis at different time windows, we propose a working model that RARβ signaling plays a crucial role in setting up the population sizes of S compartments along the rostrocaudal axis (Fig. 6). Under physiological conditions, the early-born S cells, due to deficiency of RA at their neurogenesis at E10.5–E11.5, develop into a small S compartment in the caudal striatum. Subsequently, elevated concentration of RA at E12.5–E13.5 LGE may enable full activation of RARβ signaling in late-born S cells, which leads to preferential expansion of the late-born S cell population. The late-born S cell population eventually evolves to form a fully blown S compartment in the rostral striatum.

Potential Involvement of the Rostral S Compartment in Neural Circuits of Psychomotor Function. The enlarged S compartment by RARβ signaling in the rostral striatum should presumably have topographically functional significance. Challenging the RAR$\beta^{-/-}$ mutant mice with apomorphine revealed a differentially responsive profile of various stereotypic behaviors, including exaggeration of head-bobbing movement and reduction of rearing activity. These behavioral phenotypes were unlikely due to changes of dopamine receptors in the mutant striatum, because D1 and D2 receptors are not altered in RAR$\beta^{-/-}$ mutant mice (12). The behavioral phenotypes instead imply that neurons in the rostral S compartment may modulate complex neural circuits of psychomotor control. It has been proposed that unbalanced activity shifting toward increased neuronal activity in S compartment is correlated with motor stereotypic behavior (30, 31), although another study has argued that motor stereotype does not require enhanced activity in S

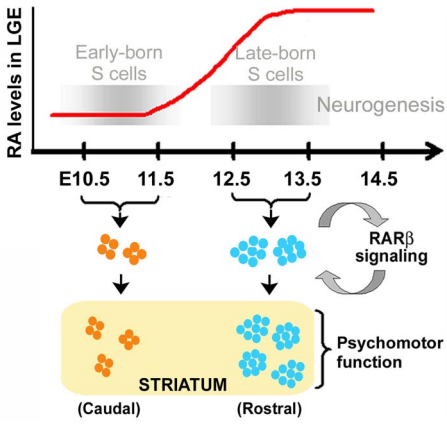

Fig. 6. Schematic drawings illustrating the working hypothesis of modular patterning of striatal compartments by RARβ signaling. The early-born S cells, because of deficiency of endogenous RA in the LGE during their neurogenesis at E10.5–E11.5, develop into a small S compartment in the caudal striatum. Subsequently elevated RA at E12.5–E13.5 enables full activation of RARβ signaling in late-born S cells, which leads to preferential expansion of the late-born S cell population. The expanded S cell population eventually evolves to form a large and elaborate S compartment in the rostral striatum, which may modulate psychomotor function. Note that, for simplicity, the effects of RA signaling on promoting differentiation of striatal neurons are omitted from the drawings.

neurons (32). The S compartment receives limbic system-associated inputs from the cerebral cortex and projects to dopaminergic neurons of the pars compacta of the substantia nigra, which may provide feedback control of dopaminergic inputs to striatal circuits (2, 3). The loss of rostral S compartment in RAR$\beta^{-/-}$ mutant striatum would conceivably result in aberrant neural circuits and perhaps change of dopamine tone within the basal ganglia, which in turn leads to altered drug-induced repetitive motor behavior. We cannot, however, rule out the possibility that there may be some uncharacterized defects in other brain regions that contribute to the behavioral phenotype of RAR$\beta^{-/-}$ mutant mice.

Aberrant RA Signaling and the Pathogenesis of Psychomotor Disorders. Clinical relevance of RA signaling in regulation of stereotypic motor behavior has been reported in patients with obsessive-compulsive disorder (OCD), because the stereotypic motor symptoms of OCD patients are alleviated with RA treatments (33). Autism, a neurodevelopmental disorder characterized by aberrant repetitive behavior, is linked to defective corticobasal ganglia circuits (34). A recent MRI study has reported a decrease in the volume of the caudate nucleus in patients with autism (35), and the etiology of autism may be associated with abnormal RA signaling and MOR deficiency (36, 37). Clinical case reports also implicate potential RA treatments for autism (38). Taken together, given that MOR1 is selectively expressed in striatal S compartments, our findings of RARβ mutation-induced aberrant S compartments and associated psychomotor dysfunction may have clinical implication for understanding the pathogenesis of autism and other psychomotor disorders.

Experimental Procedures

Detailed experimental procedures are described in *SI Text*.

Mutant Mice. RARβ mutant mice were generated (39). See *Experimental Procedures* in *SI Text*.

Immunohistochemistry. Immunohistochemistry was performed as described (40) with the following primary antibodies: rabbit MOR1 [1:10,000, gift of R. P. Elde (University of Minnesota, Minneapolis)] mouse calbindin (1:500, Sigma), rabbit met-enkephalin (1:2,000, gift of R. P. Elde), rabbit DARPP-32 (1:150, Cell Signaling), rabbit tyrosine hydroxylase (1:2,000, EugenTech), rabbit Ki67 (1:200, NovoCastra), rabbit βIII-tubulin (TuJ1, 1:1,000, Covance), sheep BrdU (1:200, Biodesign) and rabbit GluR1 (1:200, Upstate Biotechnology).

***In Situ* Hybridization.** *In situ* hybridization was performed as described (13). See *Experimental Procedures* in *SI Text*.

Cell Culture. The cultivation of explant tissue, Sil-15 RA reporter cells, and ST14 cells was performed as described (9, 20, 23). See *Experimental Procedures* in *SI Text*.

Behavioral Tests. See *Experimental Procedures* in *SI Text*.

ACKNOWLEDGMENTS. We thank R. P. Elde and E. Cattaneo (University of Milan, Milan) for reagents, D.-Y. Chen for advice on statistics, and C. P. Hung for reading the manuscript. This work was funded in part by National Health Research Institutes (Grants EX94, EX95, EX96, EX97-9402NI), National Research Program for Genomic Medicine (Grants NSC95-3112-B-010-014, NSC96-3112-B-010-007), and Ministry of Education (Aim for Top University Grant, 96A-D-T171) in Taiwan.

1. Graybiel AM, Ragsdale CW, Jr (1978) Histochemically distinct compartments in the striatum of human, monkey, and cat demonstrated by acetylthiocholinesterase staining. *Proc Natl Acad Sci USA* 75:5723–5726.
2. Graybiel AM (1990) Neurotransmitters and neuromodulators in the basal ganglia. *Trends Neurosci* 13:244–254.
3. Gerfen CR (1992) The neostriatal mosaic: multiple levels of compartmental organization. *Trends Neurosci* 15:133–139.
4. Mark M, Ghyselinck NB, Chambon P (2006) Function of retinoid nuclear receptors: Lessons from Genetic and Pharmacological Dissections of the Retinoic Acid Signaling Pathway During Mouse Embryogenesis. *Annu Rev Pharmacol Toxicol* 46:451–480.
5. Maden M (2002) Retinoid signalling in the development of the central nervous system. *Nat Rev Neurosci* 3:843–853.
6. Toresson H, Mata de Urquiza A, Fagerstrom C, Perlmann T, Campbell K (1999) Retinoids are produced by glia in the lateral ganglionic eminence and regulate striatal neuron differentiation. *Development* 126:1317–1326.
7. Smith D, Wagner E, Koul O, McCaffery P, Drager UC (2001) Retinoic acid synthesis for the developing telencephalon. *Cereb Cortex* 11:894–905.
8. Marklund M, Sjodal M, Beehler BC, Jessell TM, Edlund T, Gunhaga L (2004) Retinoic acid signalling specifies intermediate character in the developing telencephalon. *Development* 131:4323–4332.
9. Liao WL, *et al*. (2005) Retinoid signaling competence and RARbeta-mediated gene regulation in the developing mammalian telencephalon. *Dev Dyn* 232:887–900.
10. Molotkova N, Molotkov A, Duester G (2007) Role of retinoic acid during forebrain development begins late when Raldh3 generates retinoic acid in the ventral subventricular zone. *Dev Biol* 303:601–610.
11. Dolle P, Fraulob V, Kastner P, Chambon P (1994) Developmental expression of murine retinoid X receptor (RXR) genes. *Mech Dev* 45:91–104.
12. Krezel W, *et al*. (1998) Impaired locomotion and dopamine signaling in retinoid receptor mutant mice. *Science* 279:863–867.
13. Liao WL, Tsai HC, Wu CY, Liu FC (2005) Differential expression of RARbeta isoforms in the mouse striatum during development: a gradient of RARbeta2 expression along the rostrocaudal axis. *Dev Dyn* 233:584–594.
14. Garel S, Marin F, Grosschedl R, Charnay P (1999) Ebf1 controls early cell differentiation in the embryonic striatum. *Development* 126:5285–5294.
15. Graybiel AM, Hickey TL (1982) Chemospecificity of ontogenetic units in the striatum: demonstration by combining [3H] thymidine neuronography and histochemical staining. *Proc Natl Acad Sci USA* 79:198–202.
16. van der Kooy D, Fishell G (1987) Neuronal birthdate underlies the development of striatal compartments. *Brain Res* 401:155–161.
17. Song DD, Harlan RE (1994) Genesis and migration patterns of neurons forming the patch and matrix compartments of the rat striatum. *Dev Brain Res* 83:233–245.
18. Wohl CA, Weiss S (1998) Retinoic acid enhances neuronal proliferation and astroglial differentiation in cultures of CNS stem cell-derived precursors. *J Neurobiol* 37:281–290.
19. Lauper N, *et al*. (1998) Cyclin E2: a novel CDK2 partner in the late G_1 and S phases of the mammalian cell cycle. *Oncogene* 17:2637–2643.
20. Cattaneo E, Conti L (1998) Generation and characterization of embryonic striatal conditionally immortalized ST14A cells. *J Neurosci Res* 53:223–234.
21. Li H, *et al*. (2000) A retinoic acid synthesizing enzyme in ventral retina and telencephalon of the embryonic mouse. *Mech Dev* 95:283–289.
22. McCaffery P, Drager UC (1994) High levels of a retinoic-acid generating dehydrogenase in the meso-telencephalic dopamine system. *Proc Natl Acad Sci USA* 91:7772–7776.
23. Wagner W, Han B, Jessell TM (1992) Regional differences in retinoid release from embryonic neural tissue detected by an *in vitro* reporter assay. *Development* 116:55–66.
24. Krushel LA, Johnston JG, Fishell G, Tibshirani R, van der Kooy D (1993) Spatially localized neuronal cell lineages in the developing mammalian forebrain. *Neuroscience* 53:1035–1047.
25. Samad TA, Krezel W, Chambon P, Borrelli E (1997) Regulation of dopaminergic pathways by retinoids: activation of the D2 receptor promoter by members of the retinoic acid receptor- retinoid X receptor family. *Proc Natl Acad Sci USA* 94:14349–14354.
26. Valdenaire O, Maus-Moatti M, Vincent JD, Mallet J, Vernier P (1998) Retinoic acid regulates the developmental expression of dopamine D2 receptor in rat striatal primary cultures. *J Neurochem* 71:929–936.
27. Liao WL, Liu FC (2005) RARbeta isoform-specific regulation of DARPP-32 gene expression: an ectopic expression study in the developing rat telencephalon. *Eur J Neurosci* 21:3262–3268.
28. Wang H-F, Liu F-C (2005) Regulation of multiple dopamine signal transduction molecules by retinoids in the developing striatum. *Neuroscience* 134:97–105.
29. Desban M, Kemel ML, Glowinski J, Gauchy C (1993) Striatal organization of patch and matrix compartments in the rat striatum. *Neuroscience* 57:661–671.
30. Canales JJ, Graybiel AM (2000) A measure of striatal function predicts motor stereotypy. *Nat Neurosci* 3:377–383.
31. Saka E, Goodrich C, Harlan P, Madras BK, Graybiel AM (2004) Repetitive behaviors in monkeys are linked to specific striatal activation patterns. *J Neurosci* 24:7557–7565.
32. Glickstein SB, Schmauss C (2004) Focused motor stereotypies do not require enhanced activation of neurons in striosomes. *J Comp Neurol* 469:227–238.
33. Gupta MA, Schork NJ, Ellis CN (1994) Psychosocial correlates of the treatment of photodamaged skin with topical retinoic acid: a prospective controlled study. *J Am Acad Dermatol* 30:969–972.
34. Lewis MH, Tanimura Y, Lee LW, Bodfish JW (2006) Animal models of restricted repetitive behavior in autism. *Behav Brain Res* 176:66–74.
35. McAlonan GM, *et al*. (2005) Mapping the brain in autism. A voxel-based MRI study of volumetric differences and intercorrelations in autism. *Brain* 128:268–276.
36. London E, Etzel RA (2000) The environment as an etiologic factor in autism: a new direction for research. *Environ Health Perspect 108 Suppl* 3:401–404.
37. Moles A, Kieffer BL, D'Amato FR (2004) Deficit in attachment behavior in mice lacking the mu-opioid receptor gene. *Science* 304:1983–1986.
38. Megson MN (2000) Is autism a G-alpha protein defect reversible with natural vitamin A? *Med Hypotheses* 54:979–983.
39. Ghyselinck NB, *et al*. (1997) Role of the retinoic acid receptor beta (RAR beta) during mouse development. *Int J Dev Biol* 41:425–447.
40. Wang H-F, Liu F-C (2001) Developmental restriction of the LIM homeodomain transcription factor Isl-1 expression to cholinergic neurons in the striatum. *Neuroscience* 103:999–1016.

Supporting Information

Liao *et al*. 10.1073/pnas.0802109105

SI Text

Experimental Procedures

Mutant Mice. RARβ mutant mice were housed in a specific pathogen-free room with 12-hr light-dark cycle in the animal center at the National Yang-Ming University. The mutant mice were maintained by back-crossing with C57/BL6J mice. Littermate offspring of heterozygote intercrosses were used for experiments. The animal procedures of experiments were approved by the Institutional Animal Care and Use Committee of National Yang-Ming University.

Genotyping of Mutant Mice. The genotyping of mutant mice was performed by PCR with tail genomic DNA. The mouse tails were collected at 3–4 weeks after birth. Following incubation in the lysis buffer (10 mM Tris, 100 mM NaCl, 10 mM EDTA, 0.5% SDS, 250 μg/ml protease K) at 55°C overnight, the lysates were treated with RNase A for 30 min at 37°C followed by protein precipitation solution (Promega) to remove RNA and proteins. The genomic DNA was extracted by isopropanol (1:1) and dissolved in Tris-EDTA buffer for at least 2 h at 50°C. For RARβ mutant mice, three primers were used for genotyping: UD96 (5′-CCAGG CTCCT TTTTC TTCTA CCATA-3′), UD97 (5′-CTGTT TCTGT GTCAT CCATT TCCAA-3′) and UD98 (5′-AGGCC TACCC GCTTC CATTG CTCAG-3′). The PCR amplification was carried out at 94°C for 6 min followed by 35 cycles at 94°C for 30 sec, 60°C for 30 sec, and 72°C for 40 sec. An additional process at 72°C for 5 min was run at the end of the PCR. The PCR products derived from UD96/UD97 and UD96/UD98 were 275 and 300 bp, which corresponded to the wild-type (WT) and RARβ null alleles, respectively.

Administration of RA and/or 5′-bromo-deoxyuridine to Mouse Embryos. Wild-type timed-pregnant CD1 mice (National Laboratory Animal Center, Taipei, Taiwan) or timed-pregnant RARβ$^{+/-}$ mutant mice were fed by oral gavage with all-*trans* RA (5 mg/kg, Sigma) or vehicle (DMSO, Merck) every 12 h from E10.5-E11.5 or E12.5-E13.5. The RA or vehicle solutions were mixed with sunflower oil for oral gavage. Following the last treatment of RA, the pregnant mice were s.c. injected with 5′-bromo-deoxyuridine (BrdU, 50 mg/kg) 1 h before embryo harvesting. For chronic treatments of RA, timed-pregnant CD1 mice were fed by oral gavage with all-*trans* RA (5 mg/kg) or vehicle every 12 h from E11.5-E17.5. For analyzing cell proliferation in striatal anlage, timed-pregnant heterozygous mutant mice at E11.5, E12.75 or E16.5 were s.c. injected with BrdU (50 mg/kg, Sigma) 1 h before embryo harvesting. The day of plug positive was defined as E0.5. For tracing the late-born S cells, timed-pregnant heterozygous mutant mice received two s.c. injections of BrdU (100 mg/kg) at E12.75 and E13 and the labeled offspring was killed at P0 or adulthood.

Preparation of Brain Tissue. Littermates of 1.5- to 6-month-old and newborn mice were used. The mice were anesthetized by i.p. injection of sodium pentobarbital and then transcardially perfused with ice-cold 4% paraformaldehyde in 0.1 M phosphate buffer (PB, pH 7.4). The brains were postfixed in the same fixative overnight and then cryoprotected in 30% sucrose in 0.1 M PBS for at least 36 h at 4°C. The brains were sectioned at 20 μm for adult and 30 μm for newborn in the coronal plane with a freezing sliding microtome (Microtom). The sections were stored in either 0.1 M PB containing 0.1% azide or antifreezing solution containing 20% glycerol before processing for immunocytochemistry or *in situ* hybridization. For harvesting embryonic brain tissue, pregnant mice were deeply anesthetized with 3% sodium pentobarbital before abdominotomy. Embryos were removed from the uterus and kept in ice-cold PBS, and the brains were removed and immersed fixation with 4% paraformaldehyde for at least 20 h and then cryoprotected in 30% sucrose in PBS for 2 days. The brains were sectioned at 12 μm with a cryostat (Leica) or at 25 μm with a sliding microtome.

***In Situ* Hybridization.** The brain sections of wild-type and littermate mutant mice were mounted on the same slides to ensure they were processed under the same condition. The riboprobes, which included *MOR1* (GenBank accession no. L13069, nt 1281–1441), *dynorphin* (NM_019374, nt 121–488), *Ebf1* (NM_053820, nt 1847–2214), *Mash1* (M95603, 572–812), *Ccne2* (AF091432, nt 333-1056) and *Raldh3* (NM053080, nt 1204–1666) were cloned into pGEM-T-easy vector (Promega) by PCR. The RARβ1/3 probe was used as previously described (1). *In situ* hybridization was preformed with ^{35}S-UTP labeled probes except *Raldh3* which was performed with digoxigenin-labeled probes (1).

TUNEL Cell Death Assay. TUNEL staining was performed on slides using the In Situ Cell Death Detection Kit (Roche) according to the manufacturer's instructions. Briefly, the sections were rinsed 2 × 5 min with 0.1 M PBS and then incubated in 0.1 M glycine/PBS for 30 min at room temperature. After a brief rinse of 0.1 M PBS, the sections were treated with 0.1% sodium citrate buffer containing 0.1% Triton-X100 in PBS for 2 min on ice. Following 3 × 5-min rinses with PBS, the sections were incubated in the labeling solution containing 10% terminal transferase (TdT) at 37°C for 1 h to label free 3′OH ends in fragmented DNA with fluorescein-dUTP. Another set of sections was processed in parallel without TdT in the labeling solution as negative controls. The sections were counterstained with DAPI (Molecular Probes) or PI (BioVision). After examination with fluorescence microscopy, the fluorescein-dUTP signals were converted into to the visible chromogen of diaminobenzedine by incubating the sections with HRP-conjugated sheep antibody against fluorescein for 1 h following blocking with 10% sheep serum for at least 1 h. The sections were then processed with immunohistochemistry as described above.

Reverse-Transcription PCR. The ventricular zone and the mantle zone of LGE were dissected from E13.5 forebrain slices. Total RNA was prepared by guanidinium thiocyanate-phenol-chloroform extraction. Two micrograms of RNA were primed with oligo(dT) (Roche), and reversely transcribed to cDNAs by SuperScrip reverse transcriptase (Invitrogen) following the manufacturer's instructions. For PCR of each gene, the GenBank accession number, forward and reverse primers, corresponding nucleotide positions of the amplicon, annealing temperature, number of reaction cycles, and size of PCR product were as follows: RARβ (AJ002942), forward, 5′-GCTTT GAAGT GGGCA TGTCC-3′, reverse, 5′-GTCAT GGTGT CTTGC TCTGG-3′, 780-1191; 50°C, 35, 412 bp; RXRβ (NM_011306), forward, 5′-CTGCA AGGGT TTCTT CAAGC-3′, reverse, 5′-ATCCT GTCCA CAGGC ATCTC-3′, 779-1018, 55°C, 35, 240 bp; RXRγ (NM_009107), forward, 5′-TGAAG GTTGC AAAGG CTTCT-3′, reverse, 5′-CACGT TCATG TCACC GTAGG-3′, 840-1146, 55°C, 35, 307 bp; Ccne2 (AF091432), forward, 5′- ATTTA AGCTG GGCAT GT-

TCA CAGGA, reverse, 5′-TTCAC ACTCA GGTCA CTTCG ACTTC TG, 333-1056, 60°C, 27 cycles, 724 bp; DARPP-32 (AF281662), forward, 5′-AGTTA GGGGA GCTTC G, reverse, 5′-AGTTT CCATC TCTCT GGG, 68–274, 60°C, 30, 207; MAP2 (M21041), forward, 5′-CATCA TCCGC ACTCC T, reverse, 5′-CGTGG TGAGC ATTGT C, 151–461, 58°C, 35 cycles, 311 bp; actin (V01217), forward, 5′-TCATG AAGTG TGACG TTGAC ATCC-3′, reverse, 5′-CCTAG AAGCA TTTGC GGTGC ACGAT G-3′, 2727–3135; 60°C, 15, 285 bp. The PCR reactions was carried out in 10 μl mixture containing 1 μl of cDNAs, 1 $\times$ PCR buffer, 0.5 U TaqDNA polymerase (Geneaid), 0.25 mM dNTP and primers (20 ng) using a thermal cycler (Biometra, Germany). The target genes were amplified by denaturing cDNAs at 94°C for 30 sec, annealing primer at the optimal temperature for 30 sec, and extending amplicons at 72°C for 40 sec. The control for genomic DNA contamination was RT-PCR without reverse transcriptase, and no DNA band was detected under this condition.

Cell Culture. The cultivation of Sil-15 RA reporter cells was performed as described (2). The reporter cells were seeded on coverslips with density of 2×10^5 cells/cm^2 and cultured in L-15 CO_2 medium for 24 h before coculturing with explant tissues. E11.5 and E13.5 mouse brains were cut in the coronal plane with a vibratome. The lateral ganglionic eminence (LGE) was isolated from the forebrain slices and rinsed three times with SF-21 serum-free medium (3) before being cocultured with Sil-15 cells for 10 h in L15-based serum-free medium containing all-*trans* retinol (10 nM, Sigma). For assaying the RA levels in E13.5 LGE along the rostrocaudal levels, the rostral and caudal parts of E13.5 LGE were isolated from the forebrain slices and then cocultured with Sil-15 cells for 10 h. The cocultures of explants and reporter cells were fixed with 2% formaldehyde and 0.2% glutaldehyde in PBS for 5 min at room temperature, and were then processed for X-gal staining.

ST14A cells (4) were propagated at 33°C in Dulbecco's modified Eagle's medium (Invitrogen) supplemented with 3.7 g/liter $NaCO_3$ (Merck), 0.29 g/liter glutamine (Invitrogen), 100 unit/ml penicillin-stryptomycin (Invitrogen), and 10% FBS (Biological Industries). Two days after subculture, the medium was replaced with SF21 serum-free medium. A*ll-trans* RA (1 μM, Sigma) or its vehicle was added to the medium, and the cells were further cultivated for 4 days *in vitro*. For the cell proliferation assay, cells were seeded in 24-well plates (5×10^4 cells/well) and pulse-labeled with BrdU (3 μg/ml, Sigma) for 3–6 h before fixation with 4% paraformaldehyde for 30 min. Immunostaining of BrdU was performed, and the proliferation index was calculated as percentage of BrdU-positive cell number of total cells as identified by DAPI staining. For RT-PCR assay of gene expression in ST14A cells, cells were cultured in 6-well dishes (2.5×10^5 cells/well) with the same culture protocol.

Quantification. For measuring MOR1-positive striosomal areas, the photomicrographs were digitalized and loaded into the Scion Image software program (Scion). The Bregma 1.30 and 0.4 mm were selected to represent the rostral and caudal levels of the striatum, respectively (5). The left, top, and right borders of the striatum were along the inner side of the lateral ventricle, the corpus callosum, and the external capsule, respectively. To exclude the area of the nucleus accumbens, a horizontal line was drawn from the top of the anterior commissure to the bottom of the external capsule, and then a second line was drawn form the central point of the first horizontal line to the bottom of the lateral ventricle. These two lines demarcated the bottom of the dorsal striatum. The striosomal and the total striatal areas (caudoputamen) of both hemispheres were measured as duplicates, and the percentage of the striatal areas taken up by striosomes was calculated by dividing the striosomal areas with total striatal areas.

To quantify the density of calbindin-positive neurons in the rostral striatum, the number of total calbindin-positive neurons was divided by the area of the striatum. For quantifying BrdU-positive cells in the adult striatum, darkly stained BrdU-positive cells were counted in the striatal proper and the subcallosal lateral streak at the level of Bregma 1.3 mm. BrdU-positive cells in each hemisphere were counted as duplicate. For calculating proliferation index in the BrdU-positive/TuJ1-negative ventricular zone at E11.5, E12.75, and E16.5 LGE/developing striatum, the number of BrdU-positive cells were divided by the number of DAPI-positive nuclei. For estimating the degree of programmed cell death, TUNEL-positive cells were counted every 100 μm along the rostrocaudal levels at E12.75, E13.5, E14.5, and E15.5 LGE/developing striatum, and the number of TUNEL-positive cells at each level were summed up for statistical analysis between genotypes.

For densitometry measurement of ^{35}S-labeled mRNA signals in x-ray film, the autoradiographic brain images in x-ray film were digitized and loaded into the Scion Image software program. The mean density of autoradiogram was measured from selective brain regions. The specific signal intensity was obtained by dividing the intensity of autoradiogram with background levels taken from the corpus callosum, and the specific signals from the selected brain regions in two hemispheres were calculated as duplicate. The intensities of the specific signals from different brains were averaged, and were then expressed as ratio relative to that of wild-type brains. Statistical analyses were performed by Student's *t* test.

Behavioral Tests. Mice (4- to 6-months old) were used in the present study ($n = 9$ for wild-type mice, $n = 10$ for RAR$\beta^{-/-}$ mutant mice). The behavioral experiments adopted the within-subject experimental design. Apomorphine (3 mg/kg, Sigma) dissolved in the vehicle of 0.2% ascorbic acid (Sigma) was s.c. administrated at 1 h after vehicle injection to each animal. A dose-response pilot study was first performed to determine the dosage of apomorphine used in the present study. Apomorphine at the dose of 3 mg/kg did not effectively elicit motor stereotypy in wild-type mice, although it significantly increased locomotor activity. The dosage of 3 mg/kg was used throughout the experiments. The behavioral responses of each animal were video-recorded for 3 min at the time points of 20 min and 50 min after the injection of vehicle or apomorphine. The number of head bobbing (repetitive stretching or swaying of the head in a back-and-forth or left-and-right motion) was counted during the last 2 min of each video clip. Locomotor activity was assessed by calculating the percentage of time excluding the stationary phases during the last 2-min period of each video clip. Rearing and grooming activity was measured by calculating the percentage of time that the animals displayed each behavior during the last 2-min period of each video clip. Data were analyzed with two-way ANOVA followed by Bonferroni's post hoc test.

1. Liao WL, Tsai HC, Wu CY, Liu FC (2005) Differential expression of RARbeta isoforms in the mouse striatum during development: a gradient of RARbeta2 expression along the rostrocaudal axis. *Dev Dyn* 233:584–594.
2. Wagner W, Han B, Jessell TM (1992) Regional differences in retinoid release from embryonic neural tissue detected by an in vitro reporter assay. *Development* 116:55–66.
3. Segal RA, Takahashi H, McKay RDG (1992) Changes in neurotrophin responsiveness during the development of cerebellar granule neurons. *Neuron* 9:1041–1052.
4. Cattaneo E, Conti L (1998) Generation and characterization of embryonic striatal conditionally immortalized ST14A cells. *J Neurosci Res* 53:223–234.
5. Hof PR, Young WG, Bloom FE, Belichenko PV, Celio MR (2000) *Comparative Cytoarchitectonic Atlas of the C57BL/6 and 129/Sv Mouse Brains* (Elsevier Science, Amsterdam).

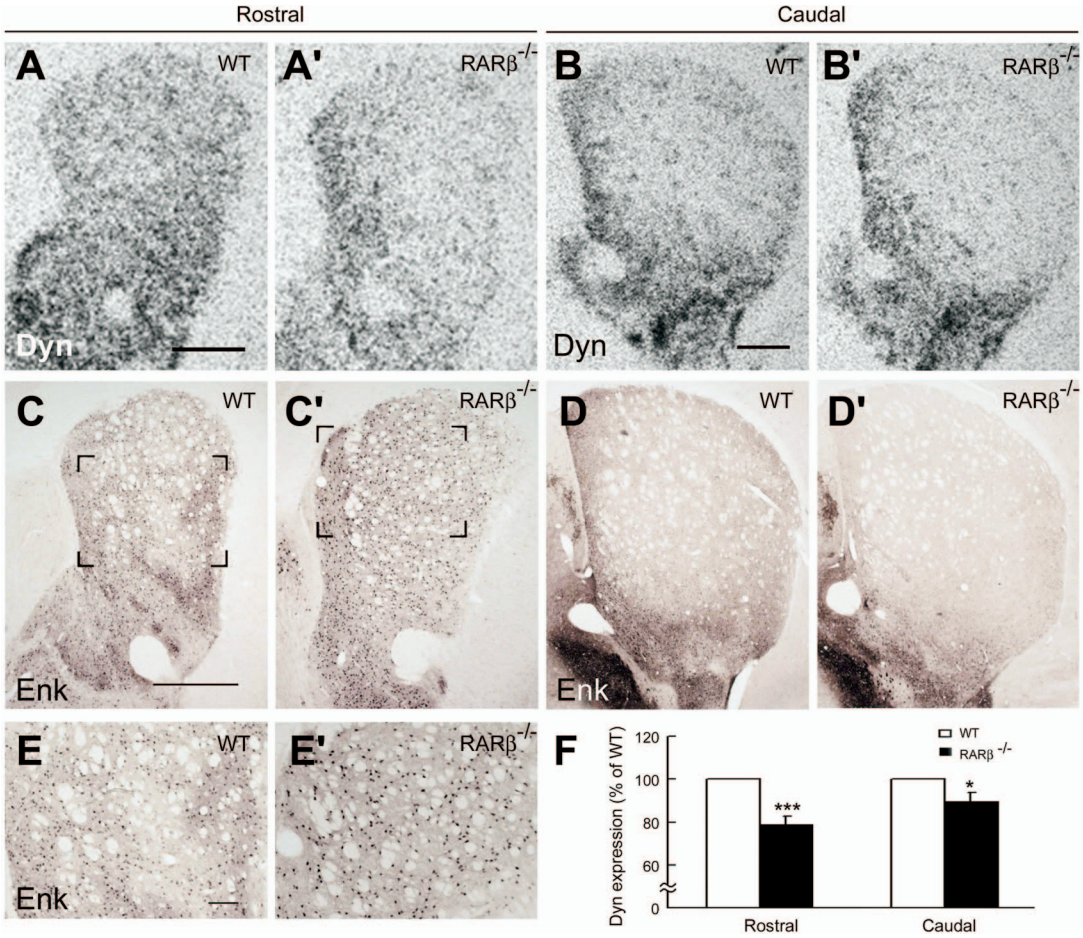

Fig. S1. Aberrant neurochemical expression in striatal compartments of adult RAR$\beta^{-/-}$ mutant mice. (*A*, *A′*, *B*, *B′*): *Dynorphin* (Dyn) mRNA, which is enriched in striosomes, is reduced by 20.95% in RAR$\beta^{-/-}$ mutant striatum at the rostral level compared with wild type striatum (*A*, *A′*, *F*). Less effect of 10.32% reduction was observed in the caudal striatum (*B*, *B′*, *F*). (*C*–*E′*): Met-enkephalin immunostaining, which is heterogeneous in wild-type striatum (*C*, *D*), appears homogenously in RAR$\beta^{-/-}$ mutant striatum at rostral levels (*C′*). The bracketed regions in *C*, *C′* are shown at high magnification in *E*, *E′*, respectively. Note that the enkephalin-poor zones, which mark the loci of striosomes (*E*), disappear in the mutant striatum (*E′*). *, $P < 0.05$; ***, $P < 0.001$, Student's *t* test, $n = 4$. (Scale bars in *A* for *A*, *A′*, 500 μm; in *B* for *B*, *B′*, *D*, *D′*, 500 μm; in *C* for *C*, *C′*, 500 μm; in *E* for *E*, *E′*, 200 μm.)

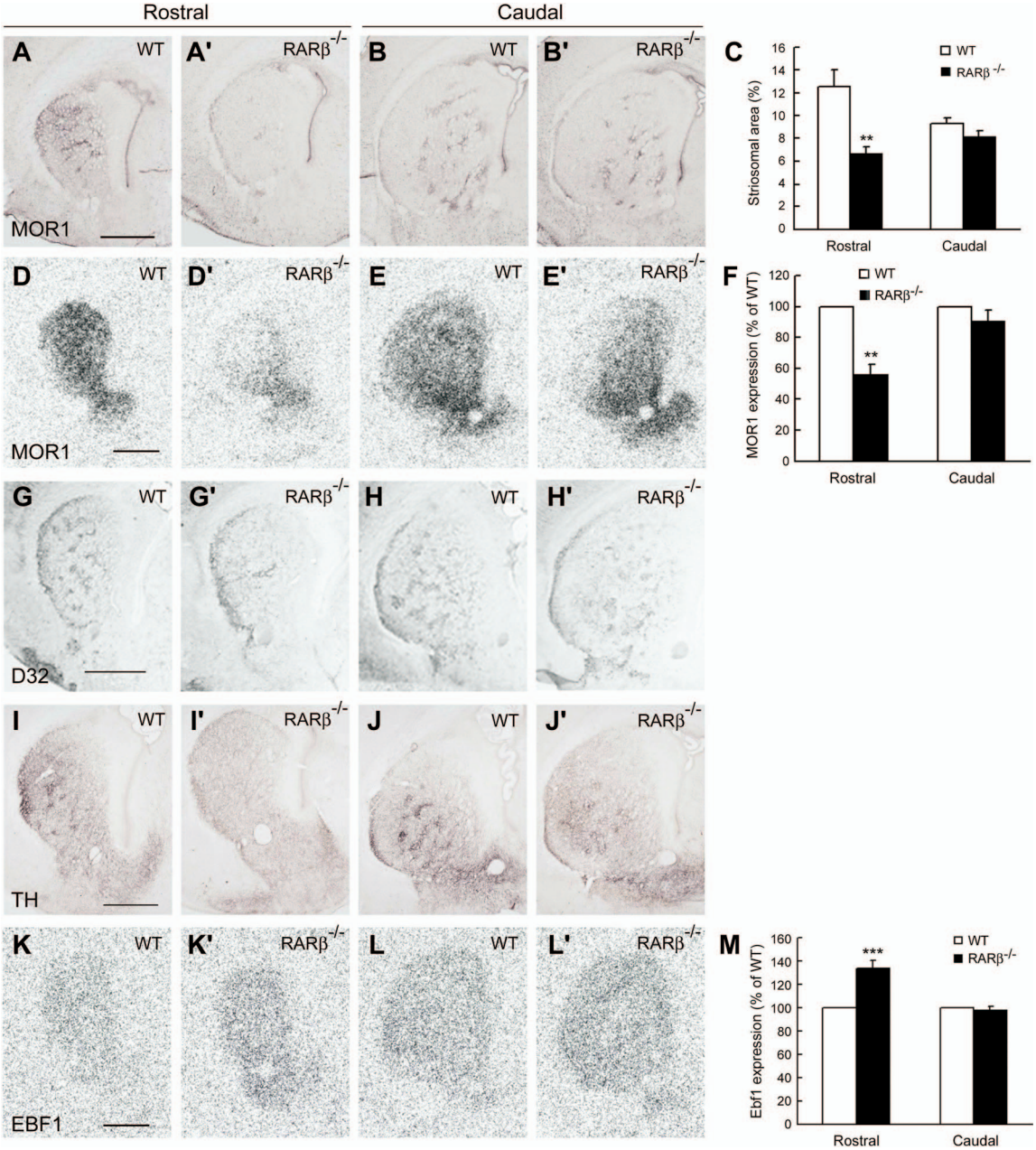

Fig. S2. Abnormal neurochemical expression in striatal compartments of newborn (postnatal day 0) RAR$\beta^{-/-}$ mutant mice. Developing striosomes containing high levels of MOR1 (*A*), DARPP-32 (D32, *G*), tyrosine hydroxylase (TH) immunoreactivity (I) and MOR1 mRNA (*D*) are diminished in RAR$\beta^{-/-}$ mutant striatum at rostral levels (*A′*, *G′*, *I′*, *D′*), whereas no significant change is observed in the mutant striatum at caudal levels except the lateral parts (*B′*, *H′*, *J′*, *E′*). The areas of MOR1-immunoreactive striosomes are reduced by 45.5% in the newborn mutant striatum at rostral levels, but no significance change was found at caudal levels (*C*). The MOR1 mRNA was also reduced by 44.1% in the newborn mutant striatum at rostral levels, but no significance alteration was found at caudal levels (*F*). (*K–M*) *Ebf1* mRNA, which is preferentially expressed by matrix cells, is increased by 33.5% in RAR$\beta^{-/-}$ mutant striatum at rostral levels (*K*, *K′*, *M*) without significant change at caudal levels (*L*, *L′*, *M*). **, $P < 0.01$, ***, $P < 0.001$, Student's *t* test, $n = 3$. (Scale bars in *A*, *P*, *G*, *I*, *K* are 500 μm for *A-B′*, *D-E′*, *G-H′*, *I-J′*, *K-L′*, respectively.)

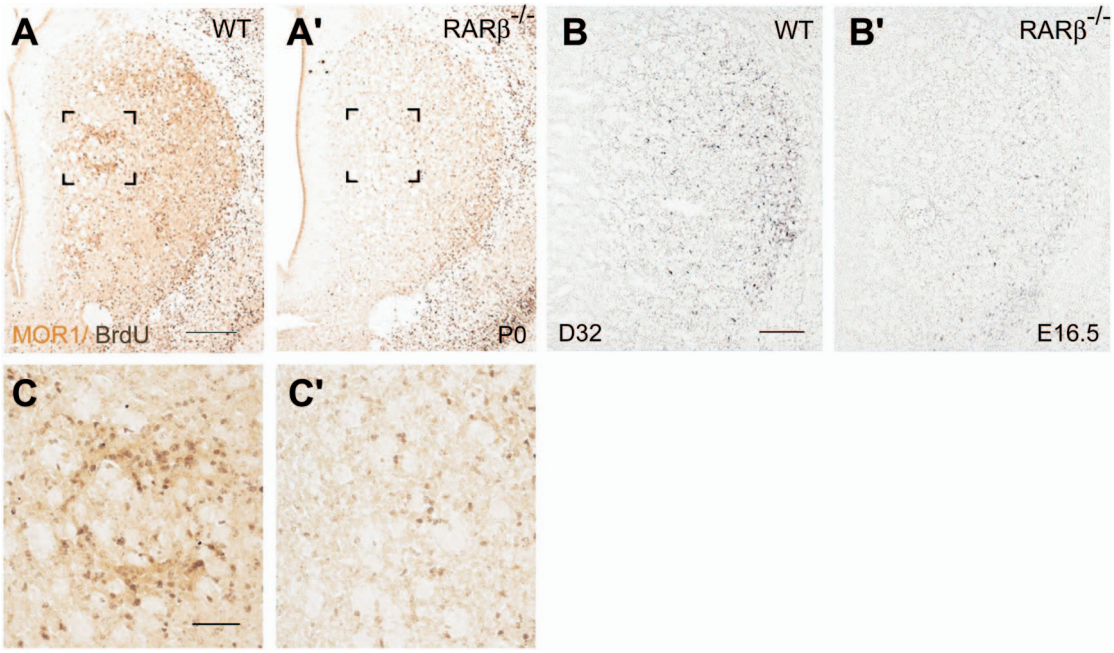

Fig. S3. Loss of late-born striosomal cells (S cells) in newborn and embryonic striatum of RAR$\beta^{-/-}$ mutant mice. (*A*, *A*′, *C*, *C*′) Double immunostaining of BrdU and MOR1 shows that typical clusters of S cells pulse-labeled with BrdU at E12.75 and E13 are present in the postnatal day 0 (P0) wild-type striatum (*A*, *C*). In contrast, few clusters of BrdU-positive cells are present in the P0 mutant striatum (*A*′, *C*′). The bracketed regions in *A*, *A*′ are shown at high magnification in *C*, *C*′, respectively. (*B*, *B*′): Before compartmental segregation at E16.5, DARPP-32-positive striosomal cells are evenly distributed in the lateral parts of both the wild type (*B*) and the mutant striatum (*B*′), but the numbers of DARPP-32-positive cells are decreased in the mutant striatum (*B*′) as compared with that in the wild-type striatum (*B*). (Scale bars in *A* for *A*, *A*′, 200 μm; in *B* for *B*, *B*′, 100 μm; in *C* for *C*, *C*′, 50 μm.)

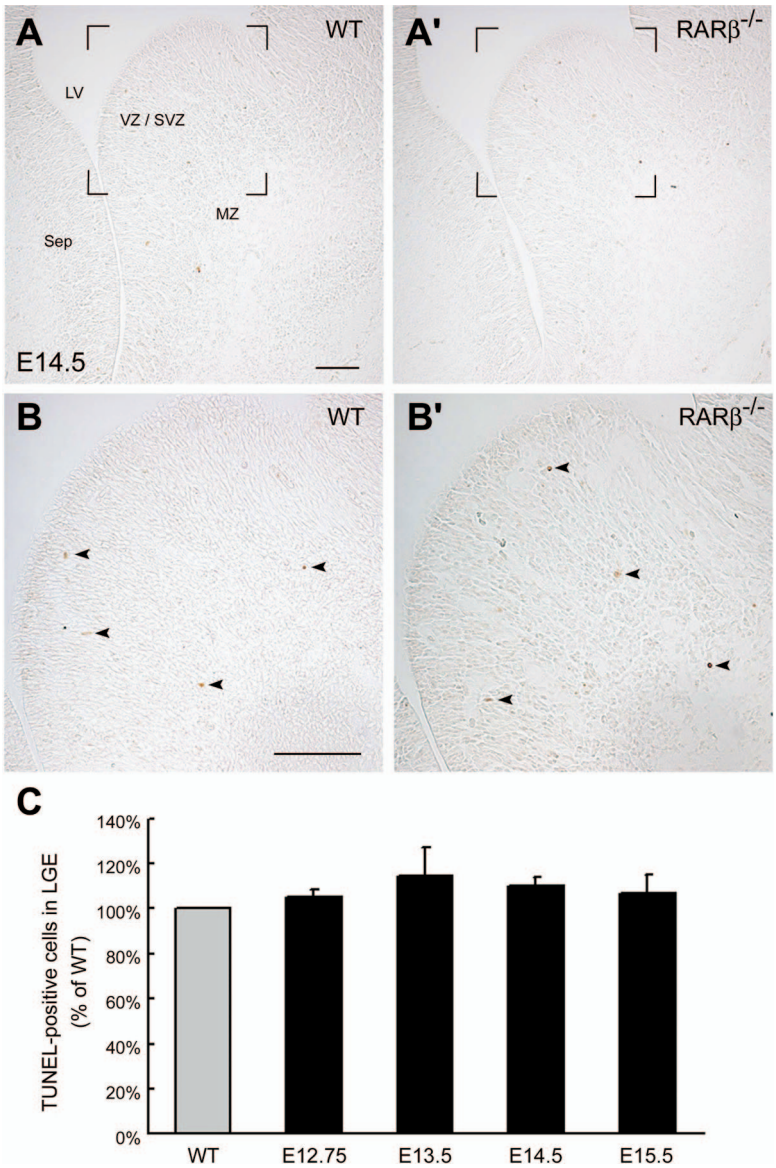

Fig. S4. TUNEL assay for cell death in striatal anlage of RAR$\beta^{-/-}$ mutant mice. (*A*-*B*′) E14.5 forebrain tissue containing the LGE (striatal anlage) were processed with TUNEL staining to assay programmed cell death. A few scattered TUNEL-positive cells are found in the LGE (arrowheads in *B*, *B*′). There is no apparent difference in the numbers of TUNEL-positive cells between the wild type (*A*, *B*) and mutant LGE (*A*′, *B*′). The bracketed region in *A*, *A*′ are shown at high magnification in *B*, *B*′. (*C*) Quantitative measurement of TUNEL-positive cells in the LGE at different embryonic stages. No significant change of the numbers of TUNEL-positive cells, as compared with the wild type LGE, is found in RAR$\beta^{-/-}$ mutant LGE at E12.75, E13.5, E14.5, and E15.5. LV, lateral ventricle; MZ, mantle zone; Sep, septum; SVZ, subventricular zone; VZ, ventricular zone. Data are representative of $n = 3$ for each embryonic stage. (Scale bars in *A* for *A*, *A*′, 200 μm; in *B* for *B*, *B*′, 100 μm.)

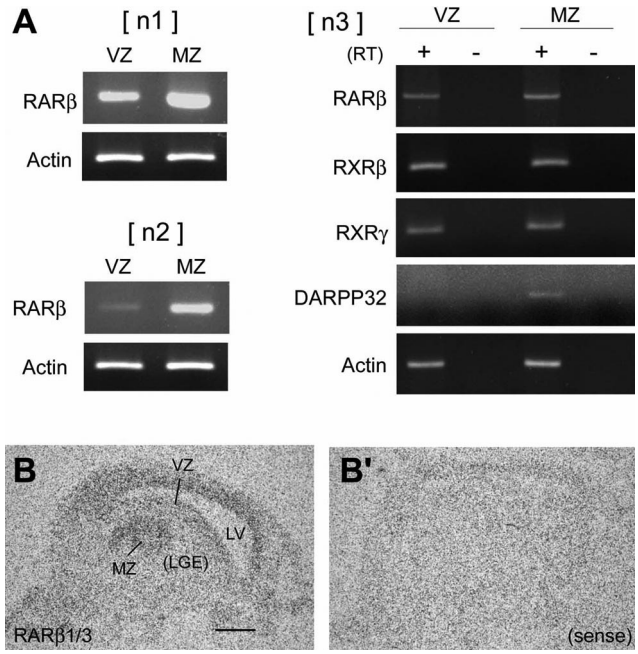

Fig. S5. Expression of RARβ mRNA in the ventricular zone of E13.5 LGE. (*A*) RARβ, RXRβ, and RXRγ mRNAs are detected in both the proliferating ventricular zone (VZ) and the differentiated mantle zone (MZ) of E13.5 LGE by RT-PCR assay. Three sets of independent experiments are presented (n1, n2, n3). Low levels of RARβ transcripts are detected in the VZ as opposed to the MZ using a set of PCR primers that recognize all RARβ isoforms. To exclude the possibility that the dissected VZ tissue might have accidentally contained MZ tissue, the expression of DARPP-32, a marker for MZ, was assayed in parallel (n3). DARPP-32 is detected in the MZ, but is barely detectable in the VZ, which rules out the possibility that the positive signals of RARβ, RXRβ and RXRγ in the VZ are confound by inclusion of MZ tissue in the VZ samples. No band is detected in the RT-PCR assay without reverse transcriptase (RT-). (*B*) *In situ* hybridization with an antisense probe recognizing both RARβ1 and RARβ3 in a parasagittal E13.5 forebrain section shows that RARβ1/3 is expressed in the VZ and MZ of LGE, which is consistent with the results of RT-PCR assay (*A*). (*B′*) Hybridization with the sense probe does not produce specific signals. LV, lateral ventricle. (Scale bar in *B* for *B*, *B′*, 500 μm.)

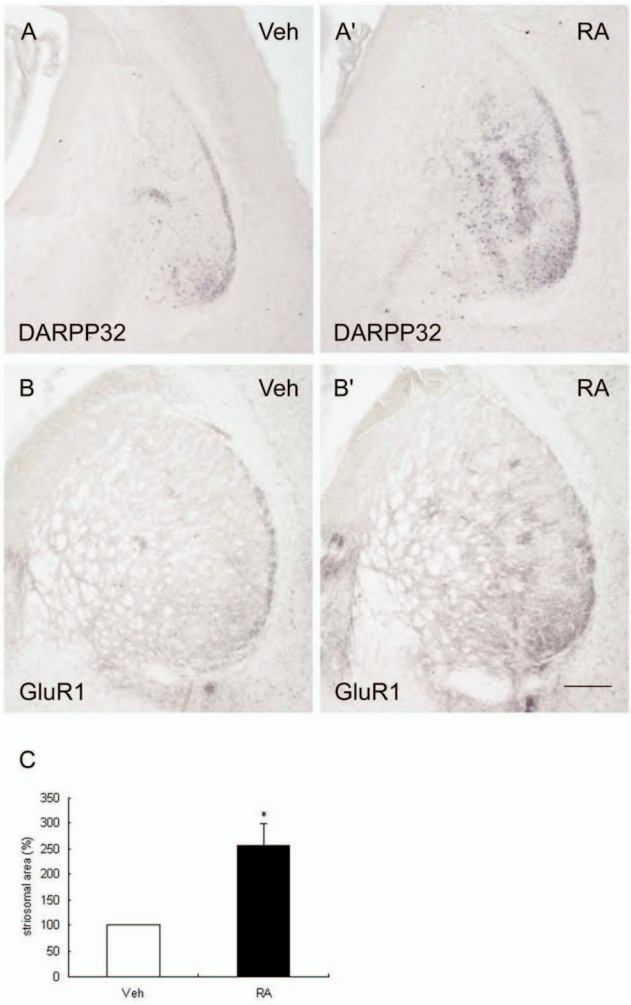

Fig. S6. Enlarged striosomes in the caudal striatum of RA-treated embryos. (*A*, *A′*) Immunostaining of DARPP-32 shows enlarged striosomes in the caudal striatum of wild-type embryos maternally treated with all-*trans* RA (5 mg/kg) every 12 h during E11.5-E17.5 (*A′*) as compared with those treated with vehicle (*A*). (*B*, *B′*) Similar results of RA-induced enlarged striosomes in the caudal striatum were found with immunostaining for GluR1, another marker for developing striosomes. (*C*) Quantitative measurement indicates GluR1-positive striosomal areas are increased by 156.3% in the caudal striatum of RA-treated embryos. *, $P < 0.05$, Student's *t* test, $n = 3$. (Scale bar in *B′* for *A*, *A′*, *B*, *B′*, 200 μm.)

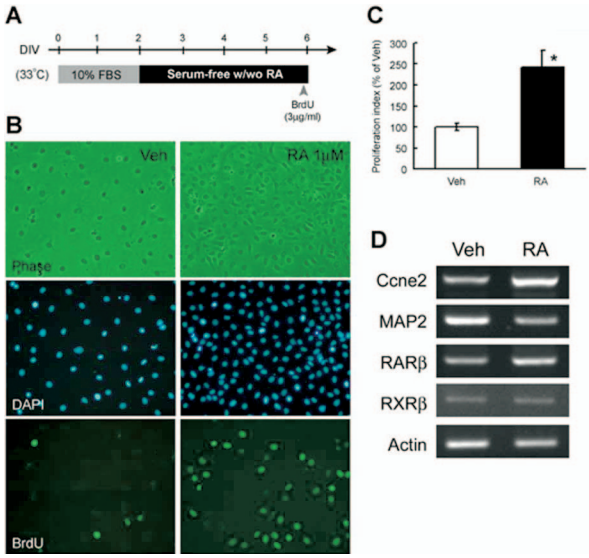

Fig. S7. Increases of proliferation of ST14A cells by RA. (*A*) ST14A cells were cultured with 10% FBS for 2 days, then cultured with serum-free medium with or without all-*trans* RA for 4 days. Cells were pulse-labeled with BrdU (3 μg/ml) before fixation. (*B*, *C*) RA increases proliferation of ST14A cells, as the percentage of BrdU-positive cells in total cells is significantly increased by RA (1 μM). (*D*) RA treatment increases Ccne2, a proliferation marker, and concurrently decreases MAP2, a differentiation marker. Note that RARβ and RXRβ are expressed in ST14A cells.